Role of stromelysin 2 (matrix metalloproteinase 10) as a novel mediator of vascular remodeling underlying pulmonary hypertension associated with systemic sclerosis

Jérôme Avouac, Christophe Guignabert, Anna Maria Hoffmann-Vold, Barbara Ruiz, Peter Dorfmuller, Sonia Pezet, Olivia Amar, Ly Tu, Jérôme van Wassenhove, Jérémy Sadoine, et al.

ARTHRITIS & RHEUMATOLOGY
Vol. 69, No. 11, November 2017, pp 2209–2221
DOI 10.1002/art.40229

Role of Stromelysin 2 (Matrix Metalloproteinase 10) as a Novel Mediator of Vascular Remodeling Underlying Pulmonary Hypertension Associated With Systemic Sclerosis

Jérôme Avouac,[1] Christophe Guignabert,[2] Anna Maria Hoffmann-Vold,[3] Barbara Ruiz,[4] Peter Dorfmuller,[2] Sonia Pezet,[4] Olivia Amar,[4] Ly Tu,[2] Jérôme Van Wassenhove,[4] Jérémy Sadoine,[5] David Launay,[6] Muriel Elhai,[1] Anne Cauvet,[4] Arun Subramaniam,[7] Robert Resnick,[7] Eric Hachulla,[6] Øyvind Molberg,[3] André Kahan,[8] Marc Humbert,[9] and Yannick Allanore[1]

Objective. **To elucidate the role of gene candidates involved in pulmonary hypertension (PH) associated with systemic sclerosis (SSc).**

Methods. **Gene candidates were identified through microarray experiments performed on Affymetrix GeneChip Human Exon 1.0 ST arrays in endothelial progenitor cell (EPC)–derived endothelial cells (ECs) obtained from patients with SSc-associated PH, patients with SSc without PH, and healthy control subjects. Expression of identified gene candidates was assessed by quantitative sandwich enzyme-linked immunosorbent assay in the serum, and by immunohistochemistry in lesional lung tissue. The functional importance of the identified gene candidates was then evaluated in *fos*-related antigen 2–transgenic (Fra-2–Tg) mice that spontaneously develop SSc-like features associated with an intense pulmonary vascular remodeling.**

Results. **Microarray experiments revealed that the matrix metalloproteinase 10 (MMP-10) gene was the top up-regulated gene in SSc-associated PH EPC-derived ECs. Circulating serum proMMP10 concentrations were markedly increased in patients with SSc-associated PH compared to SSc patients without PH and healthy controls. Consistent with these observations, a strong MMP10 staining of the thickened wall of distal pulmonary arteries was found both in the lungs of patients with SSc-associated PH and in the lungs of Fra-2–Tg mice. Daily treatment of Fra-2–Tg mice with neutralizing anti-MMP10 antibodies did not significantly affect the development and severity of pulmonary fibrosis, but did reverse established PH and markedly reduced pulmonary vascular remodeling by reducing cell proliferation, cell survival, and the platelet-derived growth factor signaling axis.**

Conclusion. **Gene expression profiling of EPC-derived ECs identified MMP10 as a novel candidate gene**

Supported by the Association des Sclérodermiques de France, INSERM, ATIP/AVENIR Program.

[1]Jérôme Avouac, MD, PhD, Muriel Elhai, MD, PhD, Yannick Allanore, MD, PhD: Université Paris Descartes, Sorbonne Paris Cité, INSERM U1016 and CNRS UMR8104, Institut Cochin, and Université Paris Descartes, Sorbonne Paris Cité, Service de Rhumatologie A, Hôpital Cochin, Paris, France; [2]Christophe Guignabert, PhD, Peter Dorfmuller, MD, PhD, Ly Tu: INSERM UMR S 999, Plessis Robinson, France, and Université Paris-Sud, Université Paris-Saclay, Le Kremlin Bicêtre, France; [3]Anna Maria Hoffmann-Vold, MD, PhD, Øyvind Molberg, MD, PhD: Oslo University Hospital–Rikshospitalet and Institute of Clinical Medicine, University of Oslo, Oslo, Norway; [4]Barbara Ruiz, Sonia Pezet, Olivia Amar, Jérôme Van Wassenhove, Anne Cauvet: Université Paris Descartes, Sorbonne Paris Cité, INSERM U1016 and CNRS UMR8104, Institut Cochin, Paris, France; [5]Jérémy Sadoine: EA 2496 Pathologie, Imagerie et Biothérapies Orofaciales, UFR Odontologie, Université Paris Descartes and PIDV, PRES Sorbonne Paris Cité, Montrouge, France; [6]David Launay, MD, PhD, Eric Hachulla, MD, PhD: Médecine Interne, Hopital Huriez, Université de Lille, Lille, France; [7]Arun Subramaniam, PhD, Robert Resnick, BS: Immunology TA, Sanofi, Framingham, Massachusetts; [8]André Kahan, MD, PhD: Université Paris Descartes, Sorbonne Paris Cité, Service de Rhumatologie A, Hôpital Cochin, Paris, France; [9]Marc Humbert, MD, PhD: INSERM UMR S 999, Plessis Robinson, France, and Université Paris-Sud, Université Paris-Saclay and AP-HP, Service de Pneumologie, Hôpital Bicêtre, Le Kremlin Bicêtre, France.

Dr. Avouac has received consulting fees from Actelion, Pfizer, and Bristol-Myers Squibb (less than $10,000 each) and research support from Roche, Pfizer, and Bristol-Myers Squibb. Dr. Humbert has received consulting fees, speaking fees, and/or honoraria from Actelion, Bayer, GlaxoSmithKline, Novartis, and Pfizer (less than $10,000 each). Dr. Allanore has received consulting fees from Actelion, Bayer, Biogen Idec, Bristol-Myers Squibb, Genentech/Roche, Inventiva, Medac, Pfizer, Sanofi/Genzyme, Servier, and UCB (less than $10,000 each) and research support from Bristol-Myers Squibb, Genentech/Roche, Inventiva, Pfizer, and Sanofi/Genzyme.

Address correspondence to Jérôme Avouac, MD, PhD, Service de Rhumatologie A, Hôpital Cochin, Université Paris Descartes, 27 Rue du Faubourg St. Jacques, 75014 Paris, France. E-mail: jerome.avouac@cch.aphp.fr.

Submitted for publication March 9, 2017; accepted in revised form August 8, 2017.

in SSc-associated PH. MMP10 is overexpressed in the serum and pulmonary arteries of patients with SSc-associated PH, and its blockade alleviates PH in the Fra-2–Tg mouse model. MMP10 appears to be a prospective treatment target for this devastating disorder.

Pulmonary hypertension (PH) is one of the leading causes of death in patients with systemic sclerosis (SSc). SSc-associated PH belongs predominantly to the World Health Organization (WHO) clinical classifications of group 1 (pulmonary arterial hypertension [PAH]) and group 3 (PH associated with interstitial lung disease [ILD]), and all recent studies have identified SSc-associated PH as one of the worst disease subsets compared to idiopathic PAH (iPAH) or all other forms of associated PH (1–3).

The current therapies for SSc-associated PH remain essentially palliative and do not reverse the progressive pulmonary vascular remodeling of the vasculature (4–6). Hence, there is a clear need for progress in the identification and validation of potential new targets for therapeutic development against this life-threatening disease.

Damage to and dysfunction of pulmonary endothelial cells (ECs) play an integral role in the initiation and progression of pulmonary vascular remodeling associated with PH (7–9). We have developed a noninvasive method to obtain cultured ECs derived from circulating endothelial progenitor cells (EPCs) (10–12). These cells have the typical EC characteristics and phenotypes, exhibit in vitro angiogenic properties, and have the capacity to constitute and orchestrate vascular remodeling in vivo (11–14). Both preclinical and clinical evidence support the notion that EPC-derived ECs may contribute to the progression of vascular complications in patients with SSc (10,11) and patients with PH (15,16). In the present study, we combined comparative transcriptome analyses of EPC-derived ECs under both normoxic and hypoxic conditions, using cells obtained from patients with SSc without PH, patients with SSc-associated PH, and healthy control subjects. In addition, we performed in vivo studies using *fos*-related antigen 2–transgenic (Fra-2–Tg) mice, an animal model that displays the main characteristic features of human SSc, specifically the development of a microvasculopathy that is paralleled by progressive pulmonary fibrosis (17–20).

Our objectives in the present study were therefore to 1) identify novel candidate genes in late-outgrowth EPC-derived ECs, under both normoxic and hypoxic conditions, from patients with SSc-associated PH (i.e., those who had precapillary PH that was confirmed by right-sided heart catheterization and who were classified as having either isolated PAH or ILD-associated PH) in comparison to SSc patients without PH and healthy controls, 2) investigate circulating concentrations and lung tissue expression of the identified gene candidates, and 3) examine the functional contributions of the identified gene candidates in vivo using the Fra-2–Tg mouse model.

MATERIALS AND METHODS

Study population. Late-outgrowth EPC-derived ECs were obtained for the purpose of this study from the peripheral blood of 46 individuals, as previously described (10,11). Thirty-six patients with SSc (28 of whom were female) whose diagnosis met the American College of Rheumatology criteria for SSc (21) were included. An extended Materials and Methods with further details on the characteristics of the patients is available upon request from the corresponding author.

Among these 36 patients with SSc, 6 had SSc and precapillary PH (SSc-associated PH), defined as precapillary PH that was confirmed by right-sided heart catheterization and a resting mean pulmonary artery pressure of ≥25 mm Hg, in conjunction with a pulmonary capillary wedge pressure of ≤15 mm Hg. Among these 6 patients with SSc-associated PH, 3 had PAH (WHO group 1) and 3 had ILD-associated PH (WHO group 3). Precapillary PH was considered secondary to ILD when the forced vital capacity was <70% of predicted, and also when the extent of fibrotic disease in the lung was >10% as determined on high-resolution computed tomography. The other 30 SSc patients without SSc-associated PH had a systolic pulmonary artery pressure of <40 mm Hg as determined on echocardiography, and a diffusing capacity for carbon monoxide of >70% of predicted. Control EPC-derived ECs were obtained from 10 healthy subjects. Details on the characteristics of all patients and controls are available upon request from the corresponding author.

Study approval. All patients and controls signed a consent form approved by the local institutional review boards (Comité de Protection des Personnes, Paris Ile de France 3). The local ethics committee (Comité d'éthique en experimentation animale 34 of Paris Descartes University) approved all animal experiments (agreement no. 15-031 [Apafis 2015080901097845 and 2015062619109294]).

Microarray analysis. Microarray analyses were performed on Affymetrix GeneChip Human Exon 1.0 ST arrays in third-passage EPC-derived ECs obtained from 6 SSc patients with precapillary PH, 20 SSc patients without PH, and 9 healthy controls. Since SSc is associated with severe tissue hypoxia, which contributes directly to its progression, gene expression profiles of EPC-derived ECs were studied both under normoxic conditions and under hypoxic conditions. In addition, we have previously reported that hypoxia modulates the gene expression profile of EPC-derived ECs in SSc (14). All microarray data and information have been submitted to the NCBI GEO database (accession no. GSE73674).

Measurement of serum proMMP10 levels. Serum concentrations of proMMP10 were measured by quantitative sandwich enzyme-linked immunosorbent assay (ELISA; R&D Systems) in accordance with the manufacturer's recommendations. Serum samples for these ELISAs were obtained from individuals in 2 independent cohorts, a discovery cohort from France and a replication cohort from Norway (22,23) (details available upon request from the corresponding author).

The French discovery cohort included 138 patients with SSc and 50 healthy controls (mean ± SD age 59 ± 15 years and 56 ± 10 years, respectively; mean ± SD duration of SSc 12 ± 9 years). Among the patients with SSc, 47 had confirmed PAH (WHO group 1), 13 had ILD-associated PH (WHO group 3), and 78 had SSc without PH. The Norwegian replication study cohort was derived from the ongoing prospective, observational Oslo University Hospital (OUH) SSc cohort study and included all individuals for whom longitudinal clinical cardiopulmonary data were available (22,23). Data were obtained from the Norwegian NOSVAR (Systemic Connective Tissue Disease and Vasculitis Registry) at OUH. This replication study sample consisted of 242 patients with SSc (mean ± SD age 48 ± 15 years; mean ± SD duration of SSc 6 ± 6 years), 42 patients with PH (30 with PAH and 12 with ILD-associated PH), and 200 without PH. Of note, for 31 of the patients with PH, including 30 with PAH and 1 with ILD-associated PH, the serum sample was obtained a mean ± SD 1.5 ± 1.92 years before the development of PH.

Detection of MMP-10 by real-time quantitative polymerase chain reaction (qPCR), Western blotting, and immunostaining. MMP-10 expression was detected by real-time qPCR, Western blotting, and immunofluorescence analyses in EPC-

Table 1. Top biologic functions and top differentially expressed genes identified by microarray analysis in patients with SSc-associated PH as compared to SSc patients without PH and healthy controls

Comparison, condition	Top biologic functions			Top differentially expressed genes (fold change)	
	Molecular and cellular function	No. of genes	*P*	Overexpressed*	Underexpressed
SSc-associated PH vs. SSc					
Basal conditions	Cell–cell signaling and interaction	4	3.16×10^{-4}–4.43×10^{-2}	MMP10 (2.197); mir-126 (1.746); PCDHB5 (1.730); TERC (1.507)	CDH2 (–3.299); ANTXR1 (–1.675); SPHAR (–1.611); ST3GAL6 (–1.604); DLG1 (–1.546); LOC645166 (–1.535)
	Cellular assembly and organization	5	3.16×10^{-4}–4.66×10^{-2}		
	Cellular function and maintenance	7	3.16×10^{-4}–4.66×10^{-2}		
	Cell cycle	1	8.07×10^{-4}–4.43×10^{-2}		
	Cell morphology	6	8.07×10^{-4}–4.66×10^{-2}		
Hypoxic conditions	Protein synthesis	3	7.07×10^{-4}–3.40×10^{-3}	CDR1 (2.479); MMP10 (2.104); mir-7 (1.720); LGALS9C (1.676); Mir-32 (1.650); OCLN (1.539); RASSF4 (1.526)	CDH2 (–2.977); GPR31 (–1.886); P2RX5 (–1.614); ST3GAL6 (–1.574); PABPN1 (–1.572); CRYAB (–1.514)
	Carbohydrate metabolism	2	8.75×10^{-4}–1.65×10^{-2}		
	Cell morphology	4	8.75×10^{-4}–4.87×10^{-2}		
	Cellular compromise	2	8.75×10^{-4}–4.37×10^{-3}		
	Energy production	1	8.75×10^{-4}–8.75×10^{-4}		
SSc-associated PH vs. healthy controls					
Basal conditions	Cell cycle	33	5.49×10^{-13}–4.93×10^{-2}	MMP10 (2.441); PLA2G4C (2.267); CYTL1 (2.092); SERPINE2 (2.047); CLIC2 (1.914); RND1 (1.628); SULF2 (1.626); ARL4C (1.515); COL4A2 (1.508); CEACAM1 (1.505)	SULT1B1 (–2.740); SLIT2 (–2.486); DPP4 (–2.247); HIST1H3A (–2.121); TOP2A (–2.106); DEPDC1 (–2.009); LDB2 (–2.001); ANLN (–1.929); KIF11 (–1.924); HIST1H1D (–1.913)
	Cellular assembly and organization	26	7.15×10^{-12}–4.93×10^{-2}		
	DNA replication, recombination, and repair	22	7.15×10^{-12}–4.93×10^{-2}		
	Cellular movement	16	8.04×10^{-9}–4.87×10^{-2}		
	Cellular function and maintenance	8	1.29×10^{-5}–4.22×10^{-2}		
Hypoxic conditions	Cell cycle	34	1.55×10^{-10}–3.42×10^{-2}	MMP10 (2.545); mir-32 (2.257); CLIC2 (2.090); TIMP3 (2.056); mir-103 (1.923); SERPINE2 (1.817); mir-7 (1.806); CD69 (1.785); RNU5B-1 (1.784); HIST1H2BJ (1.768)	SLIT2 (–2.414); SULT1B1 (–2.370); TOP2A (–2.051); LDB2 (–2.015); ASPM (–1.955); DPP4 (–1.922); GPR31 (–1.911); STEAP1 (–1.898); ANLN (–1.895); PRC1 (–1.866)
	Cellular assembly and organization	28	1.55×10^{-10}–3.42×10^{-2}		
	DNA replication, recombination, and repair	17	1.55×10^{-10}–3.42×10^{-2}		
	Cell morphology	13	8.53×10^{-5}–3.42×10^{-2}		
	Lipid metabolism	9	1.56×10^{-4}–3.42×10^{-2}		

* The gene for matrix metalloproteinase 10 was the most significantly up-regulated gene in patients with systemic sclerosis (SSc)–associated pulmonary hypertension (PH).

derived ECs (11,14). Immunofluorescence and confocal analyses for MMP10 were performed in lesional lung tissue sections obtained from patients with SSc-associated PH and Fra-2–Tg mice.

Evaluation of the effects of MMP10 inhibition in Fra-2–Tg mice. The efficacy of inhibition of MMP10 expression on the development of experimental PH and interstitial fibrosis was tested in 2 independent sets of experiments (details available upon request from the corresponding author).

In the first set of experiments, a group of 13-week-old Fra-2–Tg mice (n = 8; 4 male, 4 female) was subjected to intraperitoneal (IP) injections of rabbit polyclonal antibodies against the catalytic domain of MMP10 (Abcam) at a dose of 30 μg/kg (diluted in phosphate buffered saline [PBS], injection of 100 μl per mouse) every other day for 5 weeks. This group was compared to a control group of 13-week-old Fra-2–Tg mice (n = 7; 3 male, 4 female) treated with IP injections of a nonrelevant rabbit polyclonal IgG (Abcam) at a dose of 30 μg/kg (diluted in PBS, injection of 100 μl per mouse) every other day for 5 weeks. Two other negative control groups were used, consisting of 13-week-old C57BL/6 mice (n = 14; 6 male, 8 female) that received IP injections of either control IgG (n = 7; 4 male, 3 female) or anti-MMP10 antibody (n = 7; 3 male, 4 female).

In the second set of experiments, 4 groups of Fra-2–Tg mice (n = 7 mice per group; 4 male mice and 3 female mice per group) received IP injections of anti-MMP10 antibodies (doses

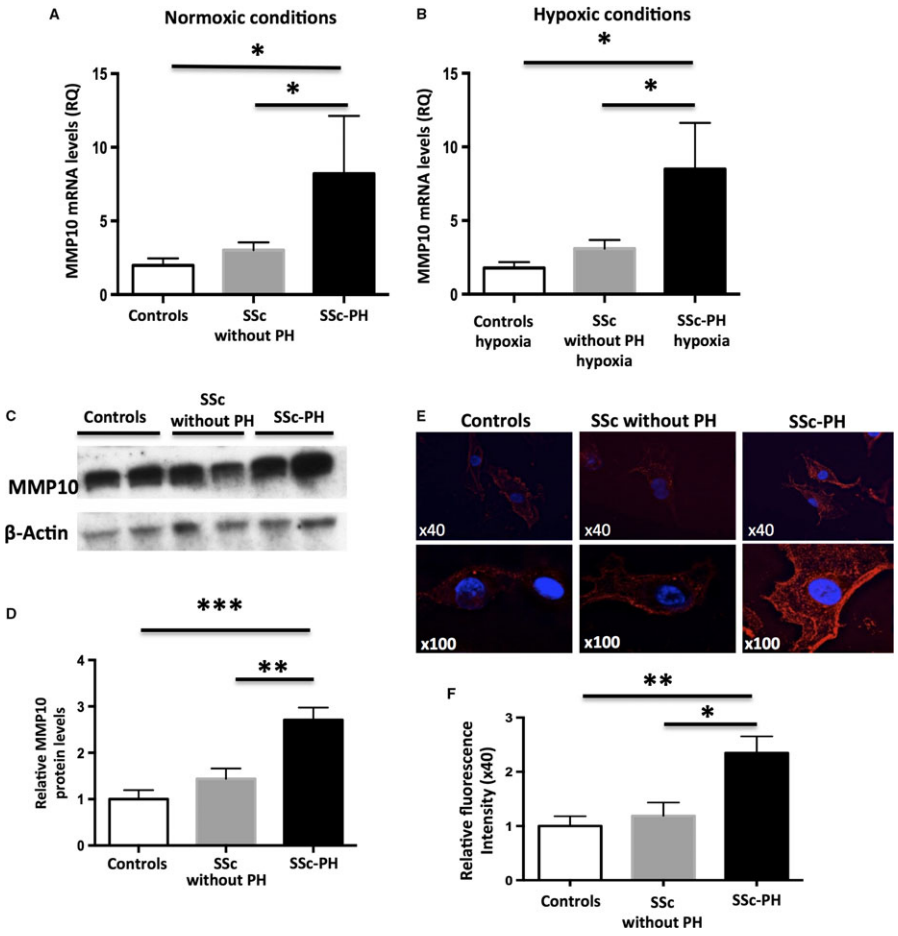

Figure 1. Increased matrix metalloproteinase 10 (MMP-10) mRNA and protein levels in circulating endothelial progenitor cell (EPC)–derived endothelial cells (ECs) from patients with pulmonary hypertension (PH) associated with systemic sclerosis (SSc). **A** and **B,** MMP10 mRNA levels (relative quantitative expression [RQ]) were assessed by real-time quantitative polymerase chain reaction in EPC-derived ECs under basal conditions **(A)** and following exposure to hypoxia **(B)**, using cells obtained from patients with SSc-associated PH, SSc patients without PH, and healthy controls. Results are the mean ± SEM in 10 control subjects, 30 SSc patients without PH, and 6 SSc patients with PH. **C,** Representative Western immunoblots show expression of MMP-10 protein (and β-actin as a control) in EPC-derived EC lysates from patients with SSc-associated PH compared to SSc patients without PH and healthy controls. **D,** Quantitative analysis of immunoblots using ImageJ software shows increased MMP-10 protein levels in SSc-associated PH EPC-derived ECs. Results are the mean ± SEM in 4 control subjects, 4 SSc patients without PH, and 4 SSc patients with PH. **E,** Representative immunofluorescence images show MMP10 localization in EPC-derived ECs from patients with SSc-associated PH compared to SSc patients without PH and healthy controls. **F,** Quantitative analysis of the immunofluorescence results using ImageJ software shows increased intensity of MMP10 immunostaining in SSc-associated PH EPC-derived ECs. Results are the mean ± SEM in 4 control subjects, 4 SSc patients without PH, and 4 SSc patients with PH. * = $P < 0.05$; ** = $P < 0.01$; *** = $P < 0.001$, by one-way analysis of variance followed by Tukey's multiple comparison test. Color figure can be viewed in the online issue, which is available at http://onlinelibrary.wiley.com/doi/10.1002/art.40229/abstract

of 30 μg/kg or 100 μg/kg), control IgG (dose of 30 μg/kg), or doxycycline (dose of 20 mg/kg), which is an antibiotic from the tetracycline family known for its ability to inhibit MMPs. Injections were administered every other day for 5 weeks.

Hemodynamic measurements and assessment of pulmonary vascular changes. The right ventricular systolic pressure (RVSP) and heart rate were determined using a closed chest technique in unventilated mice following administration of isoflurane anesthesia (2.0%, 2 liters O_2/minute). Right ventricular hypertrophy (RVH) was determined with the use of the Fulton index (24–26). Paraffin-embedded lung tissue sections were stained with hematoxylin and eosin and α-smooth muscle actin for morphometric analyses of pulmonary vascular changes (27).

Assessment of interstitial fibrosis. Fibrosing alveolitis was evaluated in all mice using micro–computed tomography (micro-CT), 2 days before the mice were killed (17). The severity of fibrosing alveolitis was semiquantitatively assessed according to the method described by Elhai et al and Ashcroft et al (17,28). The collagen content in mouse lesional lung samples was explored using an hydroxyproline assay (29,30).

Statistical analysis. All data are expressed as the mean ± SEM. Statistical analysis was performed using GraphPad Prism 6.04 software. For a 2-group comparison, unpaired or paired *t*-tests were used. One-way analysis of variance followed by Tukey's multiple comparison test was performed to compare data among 3 or more independent groups. Correlations were assessed using Spearman's rank correlation test. Predictors of the subsequent development of SSc-associated PH in the prospective Norwegian cohort were analyzed by univariate Cox proportional hazards models. Results are presented as the mean of ≥2 independent experiments, unless specified otherwise. *P* values less than 0.05 were considered significant.

RESULTS

Identification of MMP10 as a top up-regulated gene in EPC-derived ECs from SSc patients with PH. In unstimulated EPC-derived ECs from patients with SSc-associated PH, supervised gene profiling analyses identified 28 differentially expressed genes as compared to cells from SSc patients without PH, and identified 112 differentially expressed genes as compared to cells from healthy controls. Ingenuity Pathway Analysis revealed significant enrichment in functional groups related to "cellular assembly and organization," and MMP10 was among the top up-regulated genes (Table 1). Volcano plots illustrating fold differences in individual gene expression and associated *P* values (expressed as negative $\log_{10}$ values) showed that MMP10 was located at prominent coordinates, highlighting its aberrant up-regulation in EPC-derived ECs from patients with SSc-associated PH (results available upon request from the corresponding author). Similar observations were made following exposure of these cells to hypoxia (Table 1).

Real-time qPCR confirmed that MMP10 messenger RNA (mRNA) levels in unstimulated ECs from patients with SSc-associated PH were increased 2.7-fold as compared to SSc patients without PH, and were increased 4.1-fold as compared to healthy controls (Figure 1A). Similar observations were made in these cells under hypoxic conditions (Figure 1B). MMP-10 protein levels, determined using Western blotting, were substantially increased in EC lysates obtained from patients with SSc-associated PH compared to EC lysates from SSc patients without PH and healthy controls (Figures 1C and D). Endothelial MMP-10 protein expression was not different between SSc patients with PAH and SSc patients with ILD-associated PH. Immunocytofluorescence studies of the ECs revealed that overexpressed MMP10 localized to the cytoplasm (Figures 1E and F).

Elevated lung and circulating levels of MMP10 in SSc patients with PH. MMP10 overexpression in SSc-associated PH EPC-derived ECs suggests that it may be potentially implicated in the pathogenesis of SSc-associated PH. Thus, we next evaluated the expression of MMP10 in the lesional lungs of patients with SSc-associated PH and determined the cell types contributing to the production of MMP10.

Confocal microscopic analyses showed a more intense MMP10 immunoreactivity in the walls of muscularized or occluded pulmonary arteries from patients with SSc-associated PH (Figures 2A and B). Double labeling with MMP10 and either *Ulex europaeus I* lectin (as a marker of vascular endothelium), SM22 (as a marker of vascular smooth muscle), or CD68 (as a marker of macrophages) revealed that endothelium, smooth muscle, and macrophages were the major local sources of MMP10 in the lungs of patients with SSc-associated PH (Figures 2A and B).

In addition to its expression in lesional lung tissue, we assessed the circulating levels of proMMP10 in 2 independent cohorts of SSc patients. Patients with SSc-associated PH from the French discovery cohort and those from the Norwegian OUH replication cohort were more likely to have significantly higher serum proMMP10 concentrations than were SSc patients without SSc-associated PH (Figure 3A). In patients with SSc-associated PH from the French cohort, serum proMMP10 levels inversely correlated with change in the 6-minute walk distance, and also correlated with the levels of N-terminal prohormone of brain natriuretic peptide (results available upon request from the corresponding author).

Patients with PAH (WHO group 1) in the French cohort showed a trend toward higher serum proMMP10 levels when compared to SSc patients without PH, a finding that was not confirmed in the Norwegian cohort. Interestingly, serum proMMP10 levels were markedly

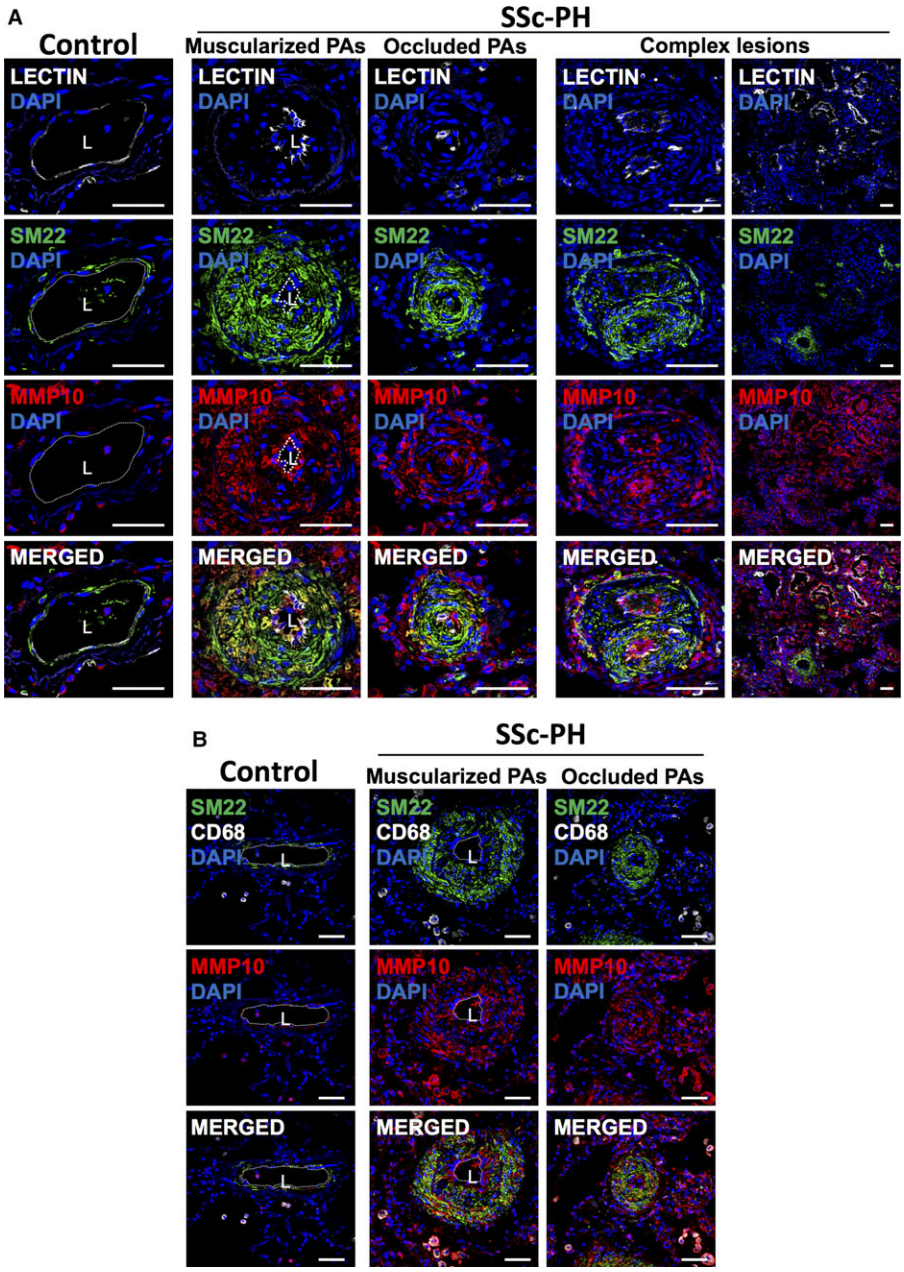

Figure 2. Overexpression of MMP10 in the pulmonary arteries (PAs) of patients with SSc-associated PH. To investigate MMP10 expression, confocal microscopic analyses were carried out by labeling with MMP10 and either *Ulex europaeus I* lectin (as a marker of vascular endothelium) or SM22 (as a marker of vascular smooth muscle) **(A)** or CD68 (as a marker of macrophages) **(B)** in human lung tissue specimens from 3 patients with SSc-associated PH and 3 healthy controls (counterstaining with DAPI). A more intense immunoreactivity was noted for MMP10 in the distal pulmonary artery walls from patients with SSc-associated PH, especially in the endothelium, smooth muscle, and macrophages. Bars = 100 μm. L = lumen (of the vessel) (see Figure 1 for other definitions).

increased in the subset of patients with ILD-associated PH (WHO group 3), both in the French cohort and in the Norwegian cohort (Figure 3B). In the combined cohort, the mean ± SEM serum proMMP10 concentration was 1,073 ± 110 pg/ml in patients with ILD-associated PH, compared to 696 ± 23 pg/ml in SSc patients without PH ($P < 0.001$) (Figure 3B) and 514 ± 92 pg/ml in patients with SSc-associated ILD without PH ($P < 0.001$). The diagnostic value of serum proMMP10 levels in patients with ILD-associated PH analyzed in the combined cohort was reflected by an area under the curve of 0.71. However, univariate Cox

proportional hazards analyses performed in the prospective Norwegian cohort did not identify serum proMMP10 levels as a predictor of the subsequent development of SSc-associated PH (hazard ratio 1.00, 95% confidence interval 0.99–1.00).

Lack of effect of MMP10 blockade on the development and severity of pulmonary fibrosis but reversal of PH in Fra-2–Tg mice. Using Fra-2–Tg mice that spontaneously develop SSc-like features associated with an intense pulmonary vascular remodeling, we first examined the expression patterns of MMP10 in the lungs, and found a substantial increase in the levels of MMP10 in the remodeled vessels of Fra-2–Tg mice, mimicking the findings in human SSc-associated PH (results available upon request from the corresponding author).

We next tested the efficacy of MMP10 inhibition on the development of pulmonary fibrosis in Fra-2–Tg mice. In the first set of experiments, micro-CT analyses showed that Fra-2–Tg mice treated with anti-MMP10 antibodies (30 μg/kg) or control IgG (30 μg/kg) had similar lung densities, and both groups had significantly higher lung density than that of wild-type C57BL/6 mice (Figures 4A and B). Furthermore, there was a loss of functional residual capacity in the lungs of Fra-2–Tg mice treated with anti-MMP10 antibodies or control IgG, a finding that was distinguishable from that in the normal lungs of wild-type control C57/BL6 mice (Figure 4C).

Lung tissue specimens from Fra-2–Tg mice treated with anti-MMP10 antibodies or with control IgG

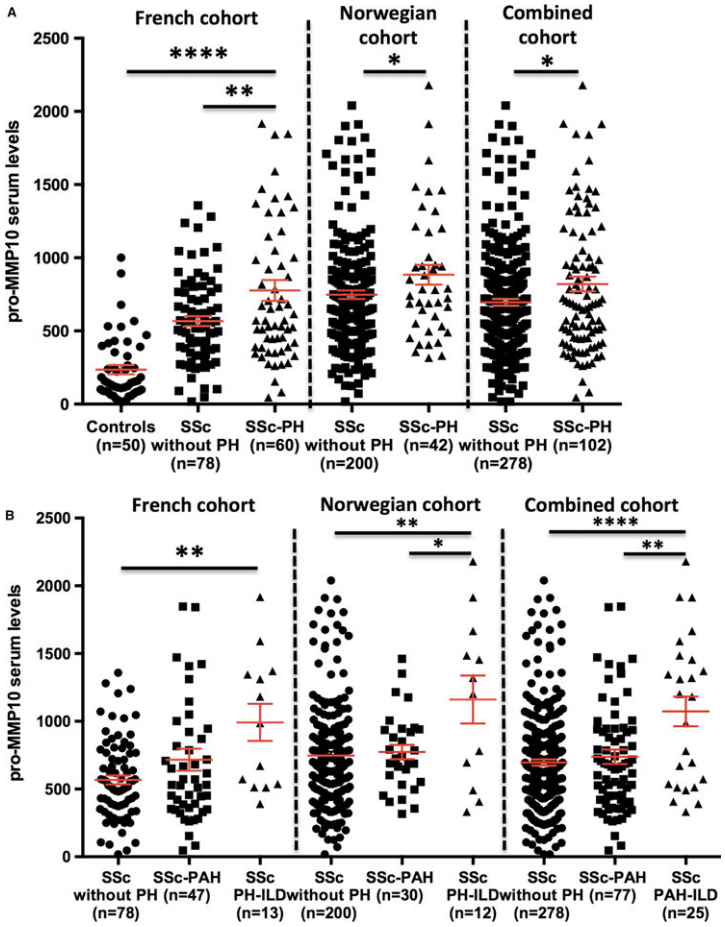

Figure 3. Elevation of serum proMMP10 levels in patients with SSc-associated PH. Serum proMMP10 levels were measured in the French discovery cohort (an observational cohort), the Norwegian replication SSc study cohort (a prospective, observational cohort from Oslo University Hospital), and the combined cohort. A marked elevation in circulating proMMP10 levels was observed in the serum of patients with SSc-associated PH **(A)**. In addition, proMMP10 concentrations were substantially increased in the subset of SSc patients with interstitial lung disease (ILD)–associated PH (World Health Organization [WHO] group 3) compared to SSc patients with pulmonary arterial hypertension (PAH) (WHO group 1) and SSc patients without PH **(B)**. Symbols show individual patients; bars show the mean ± SEM. * = $P < 0.05$; ** = $P < 0.01$; **** = $P < 0.0001$, by one-way analysis of variance followed by Tukey's multiple comparison test for comparisons of 3 groups, and Student's *t*-test for comparison of 2 groups. See Figure 1 for other definitions. Color figure can be viewed in the online issue, which is available at http://onlinelibrary.wiley.com/doi/10.1002/art.40229/abstract

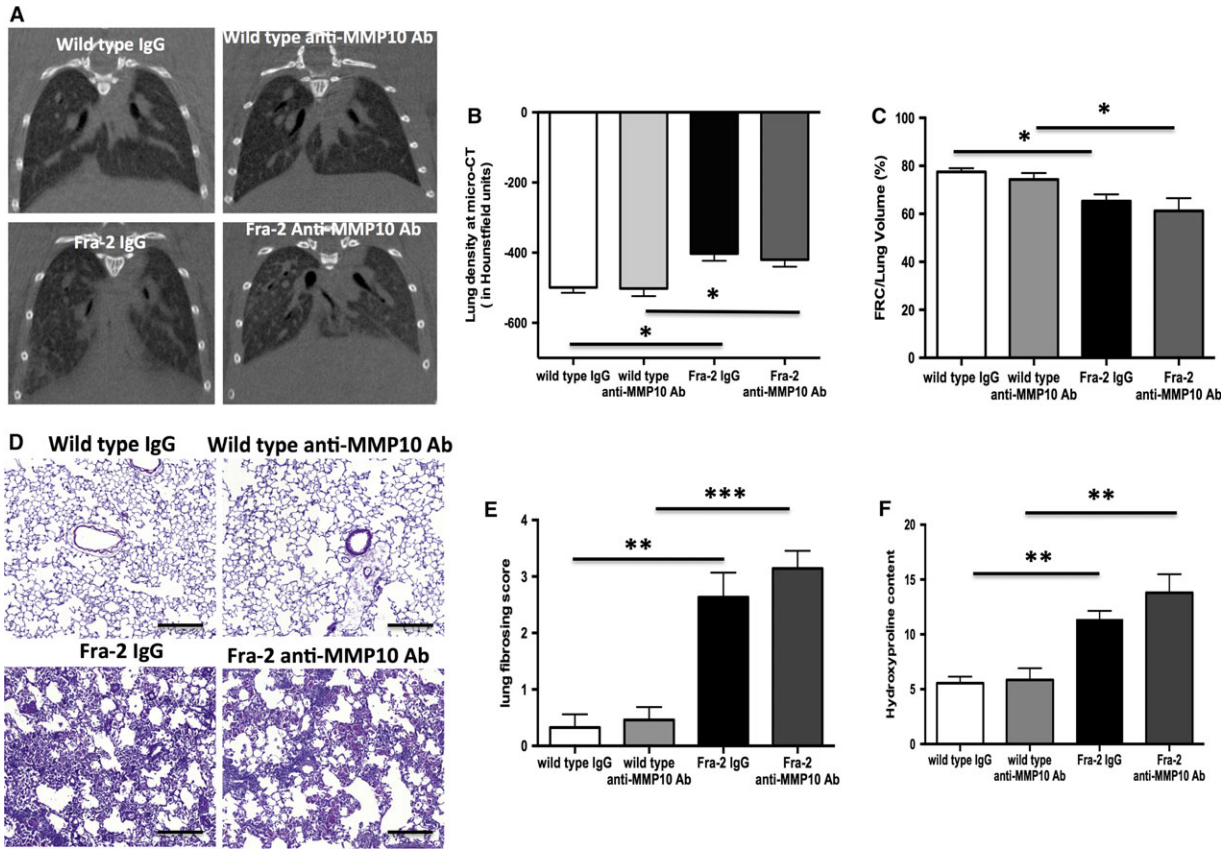

Figure 4. Evaluation of the efficacy of MMP10 inhibition through a molecular targeted strategy using antibodies (Ab) against the catalytic domain of MMP10 on the progression of lung fibrosis in *fos*-related antigen 2–transgenic (Fra-2–Tg) mice. Representative micro–computed tomography (micro-CT) images show evidence of lung fibrosis in Fra-2–Tg mice receiving anti-MMP10 antibodies or control IgG, but not in wild-type mice **(A)**. Lung density, as determined by micro-CT, is increased in Fra-2–Tg mice treated with anti-MMP10 antibodies or control IgG as compared to wild-type mice **(B)**. Residual lung volume, expressed as the percentage of functional residual capacity on total lung volume, is significantly higher in wild-type mice as compared to Fra-2–Tg mice treated with anti-MMP10 antibodies or control IgG **(C)**. Representative lung tissue specimens (stained with hematoxylin and eosin) from Fra-2–Tg mice treated with anti-MMP10 antibodies or control IgG exhibit SSc-like features of nonspecific interstitial pneumonia **(D)**. Histologic scores of lung fibrosis are significantly higher in Fra-2–Tg mice receiving anti-MMP10 antibodies or control IgG as compared to wild-type mice **(E)**. Hydroxyproline content is significantly higher in Fra-2–Tg mice treated with anti-MMP10 antibodies or control IgG as compared to wild-type mice **(F)**. In all experiments, 30 mice were analyzed. Results are the mean ± SEM. Bars = 100 μm. * = $P < 0.05$; ** = $P < 0.01$; *** = $P < 0.001$, by one-way analysis of variance followed by Tukey's multiple comparison test. See Figure 1 for other definitions. Color figure can be viewed in the online issue, which is available at http://onlinelibrary.wiley.com/doi/10.1002/art.40229/abstract

exhibited the SSc-like features of nonspecific interstitial pneumonia, with large patchy areas of lung parenchyma characterized by both diffuse cellular inflammation and collagen deposition (Figure 4D) (17). The histologic score of lung fibrosis was significantly higher in Fra-2–Tg mice treated with either anti-MMP10 antibodies or control IgG as compared to wild-type mice (Figure 4E). Consistent with the results of micro-CT analysis and histology, the hydroxyproline content was similar between Fra-2–Tg mice treated with anti-MMP10 antibodies and Fra-2–Tg mice treated with control IgG (Figure 4F).

The results obtained with the second independent set of experiments showed that MMP10 inhibition with anti-MMP10 antibodies (at doses of 30 μg/kg or 100 μg/kg) or pan-MMP inhibition with doxycycline failed to significantly improve the severity of pulmonary fibrosis in Fra-2–Tg mice. However, a slight, albeit nonsignificant, trend toward improvement in the micro-CT parameters and hydroxyproline content was observed in Fra-2–Tg mice treated with anti-MMP10 antibodies at a dose of 100 μg/kg (results available upon request from the corresponding author).

Finally, we tested the efficacy of MMP10 inhibition on the development of PH in Fra-2–Tg mice. In the first set of experiments, IgG-treated Fra-2–Tg mice, compared to wild-type mice, displayed a marked increase in the RVSP (mean ± SEM 33.7 ± 2.2 mm Hg versus 24.7 ± 2.0 mm Hg; $P < 0.001$) and in the RVH (assessed as the

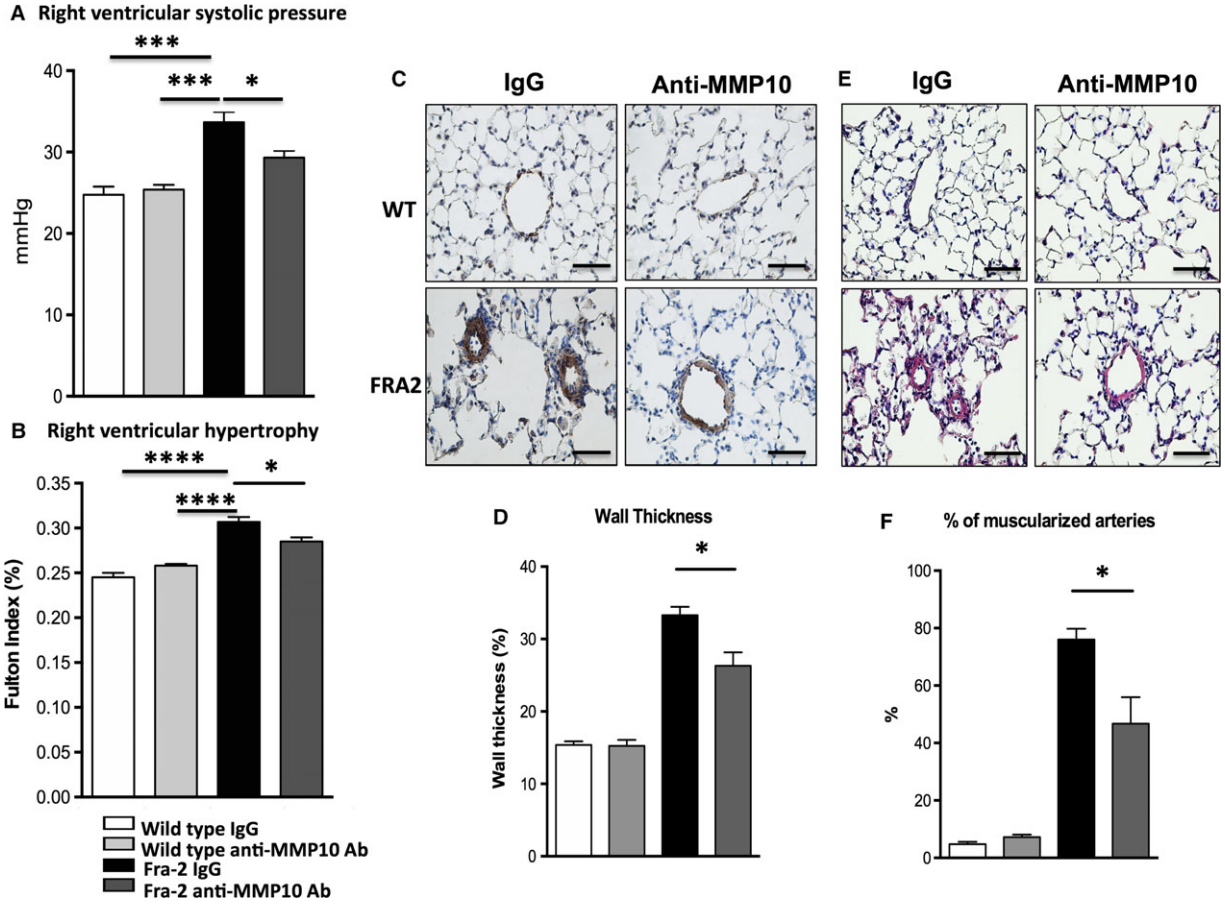

Figure 5. Evaluation of the efficacy of MMP10 inhibition through a molecular targeted strategy using antibodies (Ab) against the catalytic domain of MMP10 on the progression of pulmonary hypertension in *fos*-related antigen 2–transgenic (Fra-2–Tg) mice. **A** and **B,** The right ventricular systolic pressure **(A)** and right ventricular hypertrophy (measured as the Fulton index) **(B)** were assessed in wild-type (WT) and Fra-2–Tg mice treated with IgG or anti-MMP10 antibodies. **C** and **D,** Representative images of hematoxylin and eosin–stained lungs **(C)** and quantification of the percentage of medial wall thickness **(D)** show substantial reductions in medial wall thickness in Fra-2–Tg mice treated with anti-MMP10 antibodies when compared to Fra-2–Tg mice receiving control IgG. **E** and **F,** Representative images of immunohistostaining for α-smooth muscle actin **(E)** and quantification of the percentage of distal artery muscularization **(F)** show significant reductions in distal artery muscularization in the lungs of Fra-2–Tg mice treated with anti-MMP10 antibodies when compared to Fra-2–Tg mice receiving control IgG. Results are the mean ± SEM in 30 mice per group. Bars = 100 μm. * = $P < 0.05$; *** = $P < 0.001$; **** = $P < 0.0001$, by one-way analysis of variance followed by Tukey's multiple comparison test. See Figure 1 for other definitions. Color figure can be viewed in the online issue, which is available at http://onlinelibrary.wiley.com/doi/10.1002/art.40229/abstract

Fulton index, or percentage of muscularized arteries) (mean ± SEM 0.31 ± 0.02% versus 0.24 ± 0.01%; $P < 0.001$) (Figures 5A and B). Consistent with these findings, an increased percentage of medial wall thickness and increased numbers of muscularized distal pulmonary arteries were found in IgG-treated Fra-2–Tg mice compared to wild-type mice (Figures 5C–F).

In contrast, these pulmonary hemodynamic parameters and the degree of pulmonary vascular remodeling were substantially attenuated in Fra-2–Tg mice receiving anti-MMP10 antibodies (dose of 30 μg/kg) when compared to Fra-2–Tg mice treated with nonrelevant IgG. Indeed, in mice treated with anti-MMP10 antibodies compared to IgG-treated mice, a substantial reduction in the RVSP (mean ± SEM 29.3 ± 2.2 mm Hg versus 33.7 ± 2.2 mm Hg; $P < 0.05$) and in the Fulton index (mean ± SEM 0.28 ± 0.01% versus 0.31 ± 0.02%; $P < 0.05$) was observed (Figures 5A and B), as well as a reduced percentage of medial wall thickness and decreased numbers of muscularized distal pulmonary arteries (Figures 5C–F). The efficacy of anti-MMP10 antibodies in terms of achieving reversal of PH in Fra-2–Tg mice was further confirmed in the second independent set of experiments, with a dose-response effect observed. However, pan-MMP inhibition with doxycycline failed to significantly improve the severity of PH in the mice (results available upon request from the corresponding author).

Effects of MMP10 blockade with MMP10 neutralizing antibodies on targeting cell proliferation, cell survival, and the platelet-derived growth factor (PDGF) signaling axis. Treatment of Fra-2–Tg mice with anti-MMP10 antibodies resulted in reduced cell proliferation as compared to that in IgG-treated Fra-2–Tg mice, as measured according to the expression levels of Pcna and Ki67 mRNA in lesional lung tissue from the mice. In addition to decreased cell proliferation, increased cell apoptosis was observed, with a significant reduction in the expression of mRNA for antiapoptotic Bcl2 (results available upon request from the corresponding author).

Previous studies have implicated PDGF as a key mediator of vasculopathy in SSc-associated PH and in Fra-2–Tg mice (20,31,32). MMP10 inhibition in Fra-2–Tg mice led to a marked reduction in the levels of Pdgfb and Pdgfrb mRNA, by 59% and 35%, respectively, as compared to the levels in IgG-treated Fra-2–Tg mice (results available upon request from the corresponding author). These results are indicative of successful targeting of the PDGF signaling axis with MMP10 inhibition.

DISCUSSION

Our results provide the first experimental evidence of a transcriptional signature with differential gene expression in EPC-derived ECs between SSc patients with PH and those without PH. Among the differentially expressed genes, MMP10 was identified using this unbiased approach of transcriptomics analysis. Since MMP10 is a multifunctional MMP involved in skeletal development, wound healing, and vascular remodeling (33), we further investigated its aberrant expression in human lung and serum specimens and analyzed its functional importance using Fra-2–Tg mice. Our results indicated that MMP10 is up-regulated in the serum and the lungs of patients with SSc-associated PH. Moreover, daily treatment with neutralizing anti-MMP10 antibodies achieved regression of established PH in Fra-2–Tg mice.

Circulating progenitors may be implicated in the pathogenesis of PH. Indeed, cells expressing progenitor markers have been detected in the lung vessels of patients with iPAH (15,25,34). In addition, late-outgrowth EPC-derived ECs from patients with heritable PAH have been studied, and it has been found that they exhibit an aberrant cell phenotype (15). Furthermore, our group has reported decreased circulating EPC counts in the peripheral blood of patients with SSc-associated PH when compared to the peripheral blood of SSc patients without PH and healthy controls (10), which suggests that these cells are recruited to sites of injury. Herein, the results of the present study extend these findings and provide evidence of a transcriptional signature with differential gene expression in EPC-derived ECs between SSc patients with PH and those without PH.

We acknowledge several limitations to the current study, given the limited sample size of patients with SSc-associated PH analyzed. Indeed, the previously reported low prevalence of PH in patients with SSc (5–10%) (1) and the small number of circulating EPCs in patients with SSc-associated PH often does not allow us to obtain EPC-derived ECs from all of our patients with this complication.

Qualitative and quantitative changes in the extracellular matrix (ECM) related to a disturbed balance between MMPs and tissue inhibitors of metalloproteinases (TIMPs) have been demonstrated to play a significant role in the pathophysiology of PH (35–38) and SSc (39). In particular, the generation of fragments and the exposure of functionally important cryptic sites in collagens, laminins, elastin, or fibronectin are known to stimulate the production of matrix glycoproteins and release of growth factors that are encrypted in the ECM or from their cell membrane–bound precursors, and to facilitate pulmonary artery smooth muscle cell proliferation and contribute to their switch from a contractile to a migratory phenotype (35,37,40).

Gene expression profiling of peripheral blood mononuclear cells (PBMCs) from patients with SSc-associated PH has been previously used to decipher genes that are differentially expressed between SSc patients with PH and those without PH, and the findings have highlighted increased expression of MMP9 in those with PH, supporting the notion that development of PH is associated with active matrix-regulating genes that are involved in vascular remodeling (41). Comparison of these data to our current findings reveals that, although EPC-derived ECs and PBMCs share several top gene ontologies, many of them are specific to each cell type (results available upon request from the corresponding author), indicating that they may reflect different components of the disease. MMP9 was not significantly differentially expressed in the ECs of patients with SSc-associated PH. However, we identified up-regulation of MMP10, a multifunctional MMP that superactivates procollagenases, which are involved in skeletal development, wound healing, and vascular remodeling (33). Overexpression of MMP10 may be promoted by growth factors, including vascular endothelial growth factor (31), PDGF (35), or bone morphogenetic proteins (BMPs), especially BMP-4 (42). Our data indicated that overabundant MMP10 plays a significant role in the progression of vascular complications in SSc. Indeed, MMP10 was the single MMP significantly

overexpressed in SSc EPC-derived ECs (results available upon request from the corresponding author).

Increased MMP10 levels were detected in the serum of patients with SSc-associated PH, which is consistent with the observed increase in levels of other proMMPs or MMPs previously detected in patients with iPAH (38,43,44), and MMP10 serum levels correlated with several clinical outcomes. However, proMMP10 levels were not predictive of further occurrence of SSc-associated PH, which may be explained by the low number of incident SSc-associated PH cases in the prospective replication cohort. MMP10 expression was also found to be overabundant in perivascular macrophages and pulmonary vascular cells from the remodeled walls of distal pulmonary arteries in patients with SSc-associated PH, which is consistent with the recently reported localization of MMP10 in pulmonary arteries of patients with iPAH (38).

MMP10 inhibition also markedly alleviated the RVSP and RVH in the Fra-2–Tg mouse model, whereas pan-MMP inhibition with doxycycline failed to significantly improve these outcomes. Interestingly, the overexpression of MMP10 observed in SSc-associated PH EPC-derived ECs was not driven or amplified by hypoxic exposure, unlike several other MMPs (45).

ProMMP10 levels were markedly increased in SSc patients with ILD-associated PH (WHO group 3), suggesting that the vasculocentric process is more severe in this subset of SSc patients. However, no symmetry was observed between serum and cellular data, given that MMP10 mRNA and protein expression was driven to a similar extent in EPC-derived ECs among the 3 patients with isolated PAH and the 3 patients with ILD-associated PH. The marked up-regulation of proMMP10 levels in this subset of patients seems, rather, to be driven more by PH than by ILD per se, since patients with SSc-associated ILD without PH had no increased levels of proMMP10 in our cohort. Moreover, MMP10 inhibition failed to significantly improve the severity of fibrosing alveolitis in the Fra-2–Tg mouse model. These results are in contrast to prior observations of elevated MMP10 serum levels in patients with idiopathic pulmonary fibrosis (46).

Given the marked elevation of proMMP10 levels in patients with ILD-associated PH, it was particularly relevant to study the contribution of MMP10 to SSc-associated PH in Fra-2–Tg mice, which develop features of the peripheral vasculopathy seen in humans, including the development of PH, paralleled by a progressive pulmonary fibrosis similar to that in patients with SSc.

Our results indicate a pathophysiologic role of MMP10 in the progression of PH in Fra-2–Tg mice. First, increased MMP10 expression was detected within the walls of remodeled pulmonary arteries of Fra-2–Tg mice, consistent with the observed differential expression of different MMP subtypes in the lesional lungs in other animal models of PH (47). Second, treatment with neutralizing anti-MMP10 antibodies significantly decreased the signs of PH, which is consistent with the reversion of vascular remodeling observed upon restoration of physiologic MMP:TIMP ratios. Third, the beneficial effects of MMP10 inhibition were restricted to the progression of vascular complications in this animal model of SSc, given the failure of this strategy to improve fibrosing alveolitis.

Our data revealed that MMP10 inhibition acts through the regulation of cell proliferation and apoptosis to alleviate vascular remodeling and the signs of PH. In addition, treatment with anti-MMP10 antibodies decreased PDGF signaling, a key molecule in vascular remodeling that is also activated in the skin and lungs of Fra-2–Tg mice (20,48).

Taken together, these findings may have important clinical implications, since at the time of diagnosis of SSc-associated PH, the majority of patients have already developed some form of pathologic pulmonary arterial remodeling. Therefore, blocking MMP10 during the pathogenesis of PH or once PH is established holds promise as a therapeutic approach for this disease.

ACKNOWLEDGMENTS

We thank F. Lerourneur and F. Dumont (Plateformes de Séquençage et Génomique), M. Andrieu (Immuno-biologie), M. Favier (Morphologie/Histologie), and P. Bourdoncle (Imagerie Cellulaire) of the Institut Cochin, and C. Chaussain of the Université Paris Descartes (Faculté de Chirurgie Dentaire, Montrouge, France). We also thank R. Thuillet for valuable technical assistance.

AUTHOR CONTRIBUTIONS

All authors were involved in drafting the article or revising it critically for important intellectual content, and all authors approved the final version to be published. Dr. Avouac had full access to all of the data in the study and takes responsibility for the integrity of the data and the accuracy of the data analysis.

Study conception and design. Avouac, Guignabert, Allanore.

Acquisition of data. Avouac, Guignabert, Hoffmann-Vold, Ruiz, Dorfmuller, Pezet, Amar, Tu, Van Wassenhove, Sadoine, Launay, Elhai, Cauvet.

Analysis and interpretation of data. Avouac, Guignabert, Hoffmann-Vold, Subramaniam, Resnick, Hachulla, Molberg, Kahan, Humbert, Allanore.

ADDITIONAL DISCLOSURE

Authors Subramaniam and Resnick are employees of Sanofi Genzyme.

REFERENCES

1. Avouac J, Airo P, Meune C, Beretta L, Dieude P, Caramaschi P, et al. Prevalence of pulmonary hypertension in systemic sclerosis in European Caucasians and metaanalysis of 5 studies. J Rheumatol 2010;37:2290–8.
2. Humbert M, Sitbon O, Chaouat A, Bertocchi M, Habib G, Gressin V, et al. Survival in patients with idiopathic, familial, and anorexigen-associated pulmonary arterial hypertension in the modern management era. Circulation 2010;122:156–63.
3. Tyndall AJ, Bannert B, Vonk M, Airo P, Cozzi F, Carreira PE, et al. Causes and risk factors for death in systemic sclerosis: a study from the EULAR Scleroderma Trials and Research (EUSTAR) database. Ann Rheum Dis 2010;69:1809–15.
4. Galie N, Humbert M, Vachiery JL, Gibbs S, Lang I, Torbicki A, et al, and the Joint Task Force for the Diagnosis and Treatment of Pulmonary Hypertension of the European Society of Cardiology (ESC) and the European Respiratory Society (ERS). 2015 ESC/ERS guidelines for the diagnosis and treatment of pulmonary hypertension. Eur Respir J 2015;46:903–75.
5. Humbert M, Sitbon O, Yaici A, Montani D, O'Callaghan DS, Jais X, et al. Survival in incident and prevalent cohorts of patients with pulmonary arterial hypertension. Eur Respir J 2010;36:549–55.
6. Humbert M, Lau EM, Montani D, Jais X, Sitbon O, Simonneau G. Advances in therapeutic interventions for patients with pulmonary arterial hypertension. Circulation 2014;130:2189–208.
7. Guignabert C, Tu L, Girerd B, Ricard N, Huertas A, Montani D, et al. New molecular targets of pulmonary vascular remodeling in pulmonary arterial hypertension: importance of endothelial communication. Chest 2015;147:529–37.
8. Huertas A, Perros F, Tu L, Cohen-Kaminsky S, Montani D, Dorfmuller P, et al. Immune dysregulation and endothelial dysfunction in pulmonary arterial hypertension: a complex interplay. Circulation 2014;129:1332–40.
9. Tuder RM, Archer SL, Dorfmuller P, Erzurum SC, Guignabert C, Michelakis E, et al. Relevant issues in the pathology and pathobiology of pulmonary hypertension. J Am Coll Cardiol 2013;62 Suppl:D4–12.
10. Avouac J, Juin F, Wipff J, Couraud PO, Chiocchia G, Kahan A, et al. Circulating endothelial progenitor cells in systemic sclerosis: association with disease severity. Ann Rheum Dis 2008; 67:1455–60.
11. Avouac J, Wipff J, Goldman O, Ruiz B, Couraud PO, Chiocchia G, et al. Angiogenesis in systemic sclerosis: impaired expression of vascular endothelial growth factor receptor 1 in endothelial progenitor–derived cells under hypoxic conditions. Arthritis Rheum 2008;58:3550–61.
12. Ingram DA, Mead LE, Tanaka H, Meade V, Fenoglio A, Mortell K, et al. Identification of a novel hierarchy of endothelial progenitor cells using human peripheral and umbilical cord blood. Blood 2004;104:2752–60.
13. Sieveking DP, Buckle A, Celermajer DS, Ng MK. Strikingly different angiogenic properties of endothelial progenitor cell subpopulations: insights from a novel human angiogenesis assay. J Am Coll Cardiol 2008;51:660–8.
14. Avouac J, Cagnard N, Distler JH, Schoindre Y, Ruiz B, Couraud PO, et al. Insights into the pathogenesis of systemic sclerosis based on the gene expression profile of progenitor-derived endothelial cells. Arthritis Rheum 2011;63:3552–62.
15. Toshner M, Voswinckel R, Southwood M, Al-Lamki R, Howard LS, Marchesan D, et al. Evidence of dysfunction of endothelial progenitors in pulmonary arterial hypertension. Am J Respir Crit Care Med 2009;180:780–7.
16. Yeager ME, Frid MG, Stenmark KR. Progenitor cells in pulmonary vascular remodeling. Pulm Circ 2011;1:3–16.
17. Elhai M, Avouac J, Hoffmann-Vold AM, Ruzehaji N, Amiar O, Ruiz B, et al. OX40L blockade protects against inflammation-driven fibrosis. Proc Natl Acad Sci U S A 2016;113:E3901–10.
18. Gomez-Arroyo J, Saleem SJ, Mizuno S, Syed AA, Bogaard HJ, Abbate A, et al. A brief overview of mouse models of pulmonary arterial hypertension: problems and prospects. Am J Physiol Lung Cell Mol Physiol 2012;302:L977–91.
19. Maurer B, Busch N, Jungel A, Pileckyte M, Gay RE, Michel BA, et al. Transcription factor Fos-related antigen-2 induces progressive peripheral vasculopathy in mice closely resembling human systemic sclerosis. Circulation 2009;120:2367–76.
20. Maurer B, Reich N, Juengel A, Kriegsmann J, Gay RE, Schett G, et al. Fra-2 transgenic mice as a novel model of pulmonary hypertension associated with systemic sclerosis. Ann Rheum Dis 2012;71:1382–7.
21. Subcommittee for Scleroderma Criteria of the American Rheumatism Association Diagnostic and Therapeutic Criteria Committee. Preliminary criteria for the classification of systemic sclerosis (scleroderma). Arthritis Rheum 1980;23:581–90.
22. Hoffmann-Vold AM, Aaløkken TM, Lund MB, Garen T, Midtvedt O, Brunborg C, et al. Predictive value of serial high-resolution computed tomography analyses and concurrent lung function tests in systemic sclerosis. Arthritis Rheumatol 2015; 67:2205–12.
23. Hoffmann-Vold AM, Gunnarsson R, Garen T, Midtvedt O, Molberg O. Performance of the 2013 American College of Rheumatology/ European League Against Rheumatism classification criteria for systemic sclerosis (SSc) in large, well-defined cohorts of SSc and mixed connective tissue disease. J Rheumatol 2015;42:60–3.
24. Guignabert C, Alvira CM, Alastalo TP, Sawada H, Hansmann G, Zhao M, et al. Tie2-mediated loss of peroxisome proliferator-activated receptor-γ in mice causes PDGF receptor-β-dependent pulmonary arterial muscularization. Am J Physiol Lung Cell Mol Physiol 2009;297:L1082–90.
25. Ricard N, Tu L, Le Hiress M, Huertas A, Phan C, Thuillet R, et al. Increased pericyte coverage mediated by endothelial-derived fibroblast growth factor-2 and interleukin-6 is a source of smooth muscle-like cells in pulmonary hypertension. Circulation 2014;129:1586–97.
26. Huertas A, Tu L, Thuillet R, Le Hiress M, Phan C, Ricard N, et al. Leptin signalling system as a target for pulmonary arterial hypertension therapy. Eur Respir J 2015;45:1066–80.
27. Le Hiress M, Tu L, Ricard N, Phan C, Thuillet R, Fadel E, et al. Proinflammatory signature of the dysfunctional endothelium in pulmonary hypertension: role of the macrophage migration inhibitory factor/CD74 complex. Am J Respir Crit Care Med 2015;192:983–97.
28. Ashcroft T, Simpson JM, Timbrell V. Simple method of estimating severity of pulmonary fibrosis on a numerical scale. J Clin Pathol 1988;41:467–70.
29. Avouac J, Elhai M, Tomcik M, Ruiz B, Friese M, Piedavent M, et al. Critical role of the adhesion receptor DNAX accessory molecule-1 (DNAM-1) in the development of inflammation-driven dermal fibrosis in a mouse model of systemic sclerosis. Ann Rheum Dis 2013;72:1089–98.
30. Ponsoye M, Frantz C, Ruzehaji N, Nicco C, Elhai M, Ruiz B, et al. Treatment with abatacept prevents experimental dermal fibrosis and induces regression of established inflammation-driven fibrosis. Ann Rheum Dis 2016;75:2142–9.
31. Heo SH, Choi YJ, Ryoo HM, Cho JY. Expression profiling of ETS and MMP factors in VEGF-activated endothelial cells: role of MMP-10 in VEGF-induced angiogenesis. J Cell Physiol 2010;224:734–42.
32. Overbeek MJ, Boonstra A, Voskuyl AE, Vonk MC, Vonk-Noordegraaf A, van Berkel MP, et al. Platelet-derived growth factor receptor-β and epidermal growth factor receptor in pulmonary vasculature of systemic sclerosis-associated pulmonary arterial hypertension versus idiopathic pulmonary arterial hypertension and pulmonary veno-occlusive disease: a case-control study. Arthritis Res Ther 2011;13:R61.
33. Batra J, Robinson J, Soares AS, Fields AP, Radisky DC, Radisky ES. Matrix metalloproteinase-10 (MMP-10) interaction with tissue inhibitors of metalloproteinases TIMP-1 and TIMP-2: binding studies and crystal structure. J Biol Chem 2012;287:15935–46.

34. Montani D, Perros F, Gambaryan N, Girerd B, Dorfmuller P, Price LC, et al. C-kit-positive cells accumulate in remodeled vessels of idiopathic pulmonary arterial hypertension. Am J Respir Crit Care Med 2011;184:116–23.
35. Chelladurai P, Seeger W, Pullamsetti SS. Matrix metalloproteinases and their inhibitors in pulmonary hypertension. Eur Respir J 2012;40:766–82.
36. Matsui K, Takano Y, Yu ZX, Hi JE, Stetler-Stevenson WG, Travis WD, et al. Immunohistochemical study of endothelin-1 and matrix metalloproteinases in plexogenic pulmonary arteriopathy. Pathol Res Pract 2002;198:403–12.
37. Lepetit H, Eddahibi S, Fadel E, Frisdal E, Munaut C, Noel A, et al. Smooth muscle cell matrix metalloproteinases in idiopathic pulmonary arterial hypertension. Eur Respir J 2005;25:834–42.
38. Hoffmann J, Marsh LM, Pieper M, Stacher E, Ghanim B, Kovacs G, et al. Compartment-specific expression of collagens and their processing enzymes in intrapulmonary arteries of IPAH patients. Am J Physiol Lung Cell Mol Physiol 2015;308:L1002–13.
39. Wei P, Yang Y, Guo X, Hei N, Lai S, Assassi S, et al. Identification of an association of TNFAIP3 polymorphisms with matrix metalloproteinase expression in fibroblasts in an integrative study of systemic sclerosis–associated genetic and environmental factors. Arthritis Rheumatol 2016;68:749–60.
40. Rabinovitch M. Pathobiology of pulmonary hypertension: extracellular matrix. Clin Chest Med 2001;22:433–49, viii.
41. Grigoryev DN, Mathai SC, Fisher MR, Girgis RE, Zaiman AL, Housten-Harris T, et al. Identification of candidate genes in scleroderma-related pulmonary arterial hypertension. Transl Res 2008;151:197–207.
42. Fessing MY, Atoyan R, Shander B, Mardaryev AN, Botchkarev VV Jr, Poterlowicz K, et al. BMP signaling induces cell-type-specific changes in gene expression programs of human keratinocytes and fibroblasts. J Invest Dermatol 2010;130:398–404.
43. Martinez ML, Lopes LF, Coelho EB, Nobre F, Rocha JB, Gerlach RF, et al. Lercanidipine reduces matrix metalloproteinase-9 activity in patients with hypertension. J Cardiovasc Pharmacol 2006;47:117–22.
44. Benisty JI, Folkman J, Zurakowski D, Louis G, Rich S, Langleben D, et al. Matrix metalloproteinases in the urine of patients with pulmonary arterial hypertension. Chest 2005;128 Suppl:572S.
45. Zempo N, Koyama N, Kenagy RD, Lea HJ, Clowes AW. Regulation of vascular smooth muscle cell migration and proliferation in vitro and in injured rat arteries by a synthetic matrix metalloproteinase inhibitor. Arterioscler Thromb Vasc Biol 1996;16:28–33.
46. Sokai A, Handa T, Tanizawa K, Oga T, Uno K, Tsuruyama T, et al. Matrix metalloproteinase-10: a novel biomarker for idiopathic pulmonary fibrosis. Respir Res 2015;16:120.
47. Pullamsetti S, Krick S, Yilmaz H, Ghofrani HA, Schudt C, Weissmann N, et al. Inhaled tolafentrine reverses pulmonary vascular remodeling via inhibition of smooth muscle cell migration. Respir Res 2005;6:128.
48. Antoniu SA. Targeting PDGF pathway in pulmonary arterial hypertension. Expert Opin Ther Targets 2012;16:1055–63.